https://doi.org/10.22226/2410-3535-2023-2-104-108

On selection of advanced compositions of flame resistant magnesium alloys

S. V. Zasypkin[1], D. L. Merson[†,1], A. I. Brilevsky[1], A. I. Irtegov[2]

[†]d.merson@tltsu.ru

[1]Institute of Advanced Technologies, Togliatti State University, Togliatti, 445020, Russia
[2]LLC Solikamsk experimental metallurgical plant, Solikamsk, 618546, Russia

Magnesium alloys are among the most advanced structural materials in aviation and mechanical engineering industry due to their low density and high strength-weight ratio, but their ability to ignite at temperatures from 500°C, while actively sustaining combustion, can cause disastrous consequences even in the event of minor emergencies. This paper is intended to investigate the compositions that can enhance flame resistance of magnesium alloys. Comparison was made between ignition temperatures of commercial cast alloy ML10, LPSO-structure alloy, advanced cast alloy with rare earth metals, and variations of these alloys with different additives — agents that improve flame resistance. It has been established that the maximum flame resistance is provided by those alloys that contain both the LPSO phase and the Yb or Ca additive as agents capable of raising the ignition temperature to 1000°C or even higher.

Keywords: magnesium alloys, structure, LPSO phase, ignition temperature, oxide film.

1. Introduction

Magnesium-based alloys are classified among the most lightweight metallic structural materials, their average density is 1.9 – 2 g/cm^2 whereas that of aluminum alloys is 2.7 – 2.8 g/cm^2, however the tensile strength of commercial cast magnesium alloys reaches 260 – 275 MPa (ML8, ML10) [1], which is virtually comparable to strength properties of aluminum alloys — 275 – 295 MPa (AK7hp, AK8M) [2, 3]. For that reason, magnesium alloys are innovative and high-demand structural materials in aerospace and transport engineering. Insufficient flame resistance is one of the factors limiting their use. For example, the temperature of possible ignition for alloy ML5 is as low as 430°C, and for ML10 alloy is 550°C [4]. Such temperatures are fairly likely in the event of even ordinary emergencies and can provoke ignition of magnesium alloy products, uncontrolled flame propagation and eventually result in devastating impacts. In this regard, the problem of increasing the ignition temperature of magnesium alloys has recently been the subject of many articles. For example, the well-known KUMADAI alloys reach ignition temperatures of up to 810°C due to the addition of Ca, CaO, Ca + Y [5]. In the paper [6], the authors, in addition to calcium, also discuss the favorable effect of Be on the flame resistance, which is not a bit of news, as the procedure of adding Be in small quantities is used at Russian magnesium foundries to prevent melt oxidation during fusion. Novel Mg-4.5Gd-3.4Y-2.6Ca (wt.%) extrusion alloy in confirmed a high ignition temperature of ≈1100°C, which was attributed to the synergic effect of Y, Gd and Ca oxides, with the dominant effect of Y_2O_3 [7]. High ignition temperature (more than 1100°C) have successfully been achieved for the first time in with a high content of aluminum and calcium (for example, Mg-4Al-2Ca-0.03Be (at.%) alloys, which are produced by hot extrusion of the heat-treated cast alloys [8 – 10]. Furthermore, according to papers [11–13] addition of elements such as Y, Ce, Gd, etc. and the presence of the so-called long-period stacking-ordered structure (LPSO phase) contribute to ignition temperature rise [6]. The objective of this paper is to identify the compositions of magnesium alloy chemical make-up containing the LPSO phase, advanced from the perspective of raising the ignition temperature.

2. Experimental methods

A number of alloys were manufactured as investigated materials at the SOMZ, LLC (Solikamsk) manufacturing site based on the following considerations:

ML10 — commercial-grade cast alloy as a prototype;

Alloy #1 — Mg-Y-Zn — as a base alloy containing the LPSO phase;

Alloy #2 — Mg-Y-Zn + 0.5% Ca, i.e. a base alloy with the addition of Ca acting as an agent that raises ignition temperature;

Alloy #3 — Mg-Y-Zn + 0.5% Yb, i.e. a base alloy with the addition of Yb acting as an agent that raises ignition temperature;

Alloy #4 — Mg-Y-Zn +1.5% Gd, i.e. a base alloy with the addition of Gd acting as both a strengthening additive and an agent that raises ignition temperature;

Alloy #5 — Mg-Gd-Zn+0.5% Yb — as an alloy with a high content of rare earth metals (REM), but not containing the LPSO phase, in which Yb acts as an agent that raises the ignition temperature.

The chemical composition of manufactured alloys presented in Table 1 was determined in two ways: using

a high-precision optical emission spectrometer ARL 4460–1632 (USA), and with the use of energy-dispersive X-ray spectroscopy (EDX) on the Shimadzu EDX-8000 device.

The alloys chemical composition is shown in Table 1.

Heat treatment (HT) was carried out as follows: ML10 alloy as per the T6 mode according to OST1 90121-90; experimental alloys #1, 3–5 as per the T6 mode (homogenization annealing at 540°C temperature for 24 hours followed by quenching in hot water and aging at 200°C for 24 hours); alloy #2 as per two-stage homogenization annealing scheme at 300°C temperature for 24 hours and at 450°C for 24 hours followed by quenching and aging according to the same modes as alloys #1, 3–5. The microstructure was analyzed using a confocal laser scanning microscope (CLSM method) LEXT OLS4000 by Olympus (Japan), and also scanning electron microscope (SEM method) by Zeiss Sigma (Germany). The phase analysis was performed on the Shimadzu XRD-7000 X-ray θ-2θ diffractometer equipped with a wide-focus Cu source working at 40 kV accelerating voltage and 40 mA current. The scanning range was set at 15–75 degrees, scanning step and speed were 0.02 degrees and 0.25 degrees/min, respectively.

Brinell hardness was determined using a stationary hardness tester Time Group HB-3000B (China) on plate-shaped specimens. Uniaxial tensile tests were carried out on round fivefold specimens with the dimensions of test section ∅6×30 mm on the Tinius Olsen H50KT machine (England).

≈15 mm side cubic specimens of cast and heat-treated alloys were made for flammability tests. Such specimen was placed in a muffle furnace at room temperature and heated at a rate of 200°C/hour either until ignition or to 1000°C. Video recording of the furnace controller with thermocouple readings and a minute-by-minute photo fixation of the specimen through the furnace inspection hole was carried out concurrently with heating. The ignition temperature was determined as the calculated temperature corresponding to the minute (sequential number of the specimen photo) at which there was a sudden change in the intensity of its glow (Fig. 1).

3. Investigation results

The ML10 alloy structures both in the initial and in the heat-treated state are typical for this alloy [14]. The structure of the as-cast alloy (Fig. 2a) consists of relief grains α-Mg, the $(MgZn)_{12}Nd$ phase is located at the boundaries, the grain boundaries are wavy and ill-defined. After T6 (Fig. 2b), the solid solution grains are smoothed out, the boundaries are straightened and become better defined.

Alloys #1–4 have similar structures. In the as-cast state, these alloys differ notably in grain size, which is due to the different Zr content in the alloys, which promotes the release of $ZrMg_3$ particles [15] being the crystallization centers. The structure (Fig. 3a, 4a, c, e) is represented by the grains heterogeneous in their chemical composition and grain size, the grain boundaries are ill-defined and have massive second phase sections randomly distributed along them. Following HT (Fig. 3b, 4b, d, f), the grain size increases significantly, and the grain size nonhomogeneity decreases, concurrently the LPSO phase ($Mg_{12}YZn$) [16] is formed along the grain boundaries with small inclusions of the eutectic W-phase ($Mg_3Y_2Zn_3$) [16] (Fig. 3c, 6a). In the base composition alloy with calcium #2, unlike other base composition alloys, the grains after HT have angular geometry (Fig. 4b) rather than that close to uniaxial (Fig. 4d, f).

Visually, alloy #5 (Fig. 5a, b) has the structure similar to alloys #1–4, however, the phase composition differs

Table 1. Chemical composition of the investigated alloys (wt.%).

	Mg	Zn	Ca	Zr	Nd	Gd	Yb	Y	LPSO
ML10	Base	0.45	-	0.60	2.22	-	-	-	-
Alloy #1	Base	2.24	-	0.39	-	-	-	6.97	+
Alloy #2	Base	2.09	0.50	0.45	-	-	-	7.47	+
Alloy #3*	Base	2.61	-	0.07	-	-	0.38	6.4	+
Alloy #4*	Base	2.36	-	0.04	-	1.30	-	5.67	+
Alloy #5*	Base	1.59	-	0.32	-	11.42	0.27	-	-

* determined using the EDX method

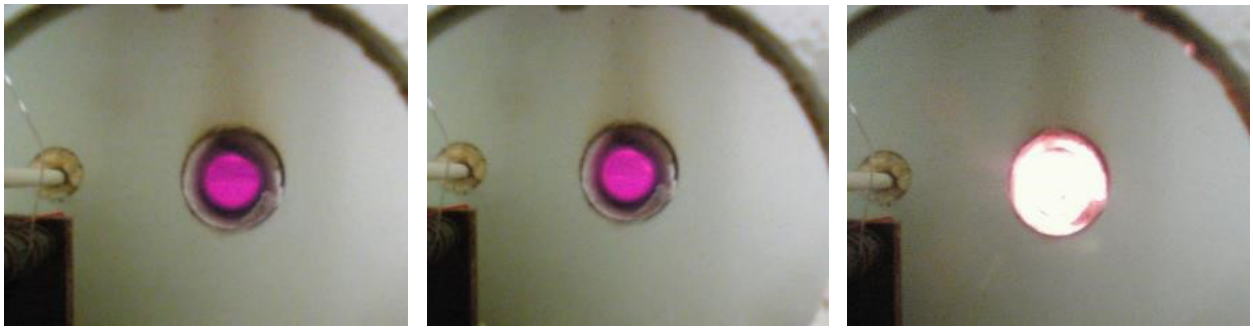

a b c

Fig. 1. (Color online) Photograph of the heat-treated ML10 specimen glow at different test minutes: 149th (a); 150th (b); 151st — a sudden change in the glow intensity (c).

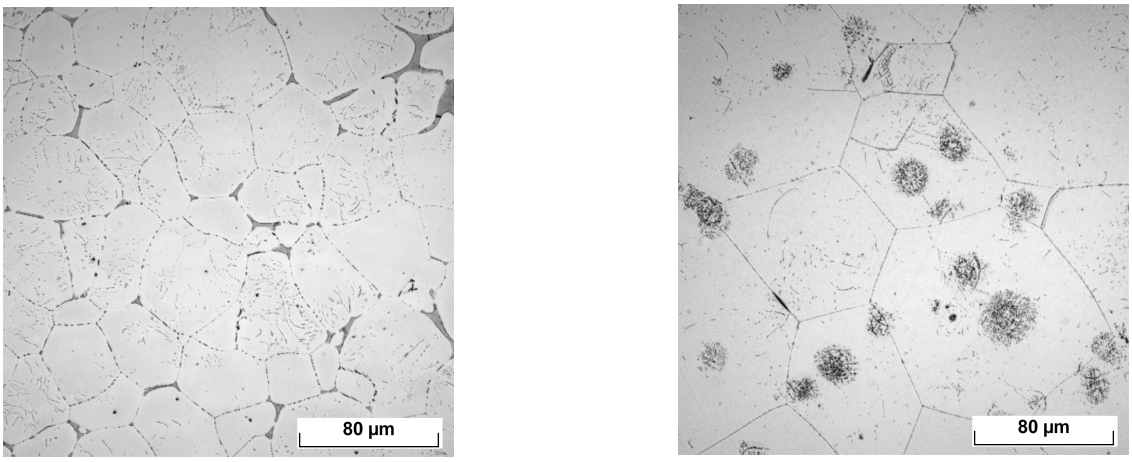

a b

Fig. 2. Microstructure of the ML10 alloy as-cast (a); after HT (b).

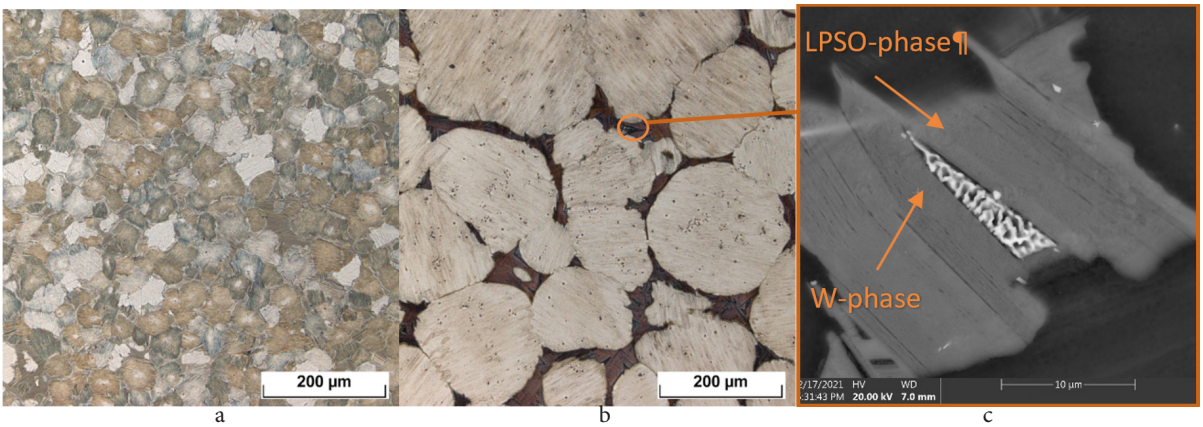

a b c

Fig. 3. (Color online) Microstructure of alloy #1 as-cast (a); after HT (b, c). (a, b) — CLSM, (c) — SEM.

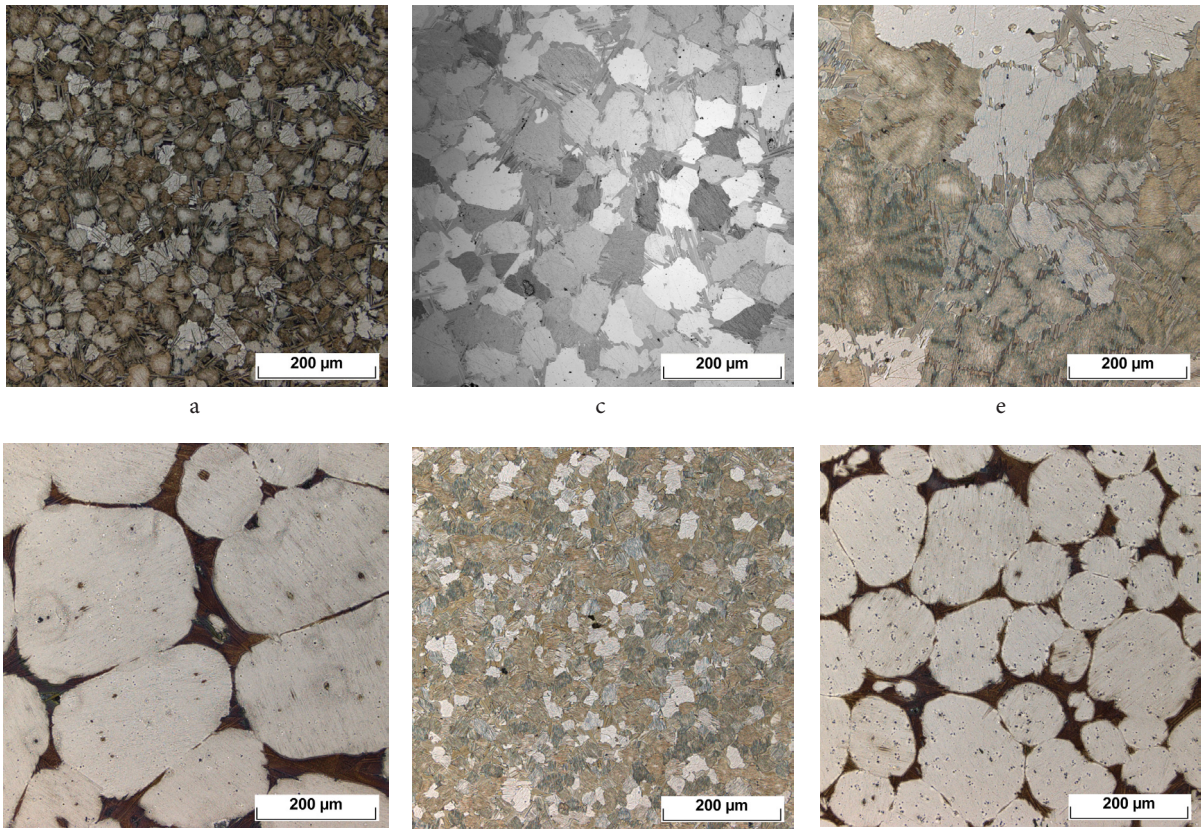

a c e

b d f

Fig. 4. (Color online) Microstructure of alloy #2 (a, b), #3 (c, d) and #4 (e, f) in the as-cast (a, c, e) and after HT (b, d, f) states. CLSM.

significantly from previous alloys. Instead of the LPSO phase, the eutectic phase $(Mg,Zn)_3Gd$ is formed at the grain boundaries (Fig. 5 c, 6 b), which significantly embrittles the alloy.

Table 2 shows the average values of mechanical characteristics based on the test results of at least two specimens of each investigated alloy in the as-cast and heat-treated (T6) states, and also the ignition temperature values.

4. Discussion

The flammability test showed (Table 2) that the presence of the LPSO phase (alloys #1-4) already in the as-cast state raises the ignition temperature T_{ignit} of magnesium alloys by at least 100°C versus the prototype alloy (ML10) (Table 2). For example, for alloy #5, with the largest REM percentage content in its composition but with no LPSO phase formation, the ignition temperature remains at the level of ML10. However, it is not just the presence of the LPSO phase that is important, but also its distribution pattern, as can be seen from the alloys #1 and 4 examples. In the as-cast state, where the alloy structure is not homogeneous and the second phases are not evenly distributed along the boundaries (Fig. 3 a, 4 e), ignition occurs at lower temperatures (765°C and 732°C for alloys #1 and # 4, respectively). After HT, the structure changes significantly, the grain boundaries mainly consist of the LPSO phase and have a considerable thickness relative to the matrix grains (Fig. 3 b, 4 f), and, as a result, T_{ignit} increases by at least 100°C (up to 862°C and 922°C for alloys #1 and #4, respectively). Should the LPSO phase be combined with "fireproof" agents (alloys #2 and 3), ignition occurs at temperatures close to 1000°C or does not occur before it altogether (Table 2). It is noteworthy that the addition of Yb to the highly-alloyed alloy #5, which contains no LPSO phase, does not have any positive effect on the T_{ignit} value.

In our view, the formation of a dense oxide film, provided it is built from the LPSO phase, plays an essential

Table 2. Mechanical properties and ignition temperature of magnesium alloys in the as-cast and heat-treated states.

	σ_B, MPa		$\sigma_{0.2}$, MPa		δ, %		HB		T_{ignit}, °C	
	C	T6	C	T6	C	T6	C	T6	C	T6
ML10	174±7	261±11	108±6	142±8	6±1.0	7±1.0	55±2	70.5±2.2	615	628
Alloy #1	197±8	244±9	131±7	169±9	6±1.0	7±1.0	66±2	69.5±2	765	862
Alloy #2	166±7	192±8	134±7	158±9	2±0.4	1±0.3	67±2	67.5±2	>1000	>1000
Alloy #3	208±8	224±9	127±7	149±8	8±1.5	5±0.8	63.5±2	67.7±2	975	>1000
Alloy #4	201±8	249±9	133±7	-	4±0.8	12±1.5	73.5±2.3	73.5±2.5	732	922
Alloy #5	227±9	262±10	-	-	3±0.6	0.8±0.2	77.5±2.5	101±4	660	630

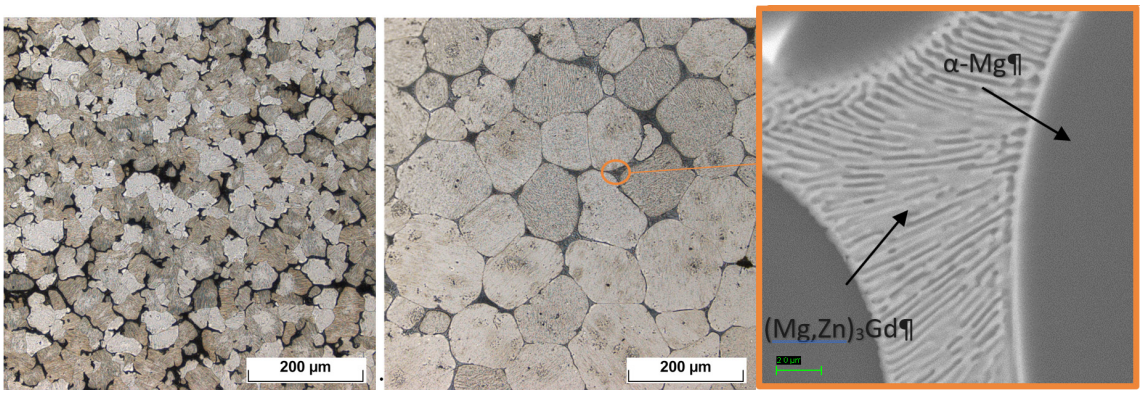

a b c

Fig. 5. (Color online) Microstructure of alloy #5 as-cast (a); after HT (b, c). (a, b) — CLSM, (c) — SEM.

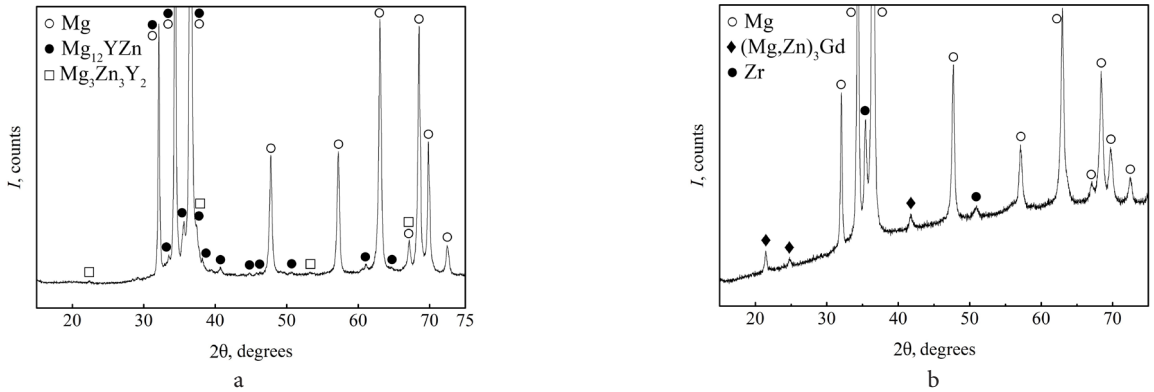

a b

Fig. 6. XRD phase analysis of alloys after heat treatment #1 (Mg-Y-Zn) (a), #5 (Mg-Zn-Gd-Yb) (b).

role in the mechanism that prevents ignition. The elements Y, Ca and Yb have a positive effect on the density and permeability of this film with oxygen and, possibly, on the rate of its formation [12,17–19]. Our future efforts will focus on understanding this subject, including the specifics of the oxide film formation mechanism, its composition and properties.

If speaking about mechanical properties, almost all alloys containing the LPSO phase, following heat treatment, have similar strength properties (at the level of 250 MPa), and the difference between them is mainly related to the difference in the average grain size, which, in turn, depends on the concentration of zirconium in the alloy. The addition of calcium, along with raising T_{ignit}, resulted in strong embrittlement and therefore, at this stage, it is excluded from the range of advanced alloying elements. The content of Zn and Y elements in alloys at 1:2.8 ratio is completely consumed to formation of the LPSO phase, which is thermally non-hardenable [20]. Based on general assumptions, with a view to further development, of greatest interest is the composition based on a base alloy with the LPSO phase (#1), completely enveloping the grains of the Mg α-phase, with the addition of Yb as an element that raises the ignition temperature, plus another element like Gd, facilitating the precipitation of dispersed particles for the mechanism of solid-solution strengthening to occur.

5. Conclusions

1. The presence of the LPSO phase in magnesium alloys raises their ignition temperature by ≈100°C in the as-cast state and by ≈200°C in the heat-treated state.
2. Making an alloy that contains the LPSO phase, Yb or Ca, allows to raise the ignition temperature of magnesium alloys to 1000°C or higher.
3. Magnesium alloys protection against ignition is largely provided by surface oxide film, which composition and formation rate may depend on the LPSO phase proportion in the alloy and on the presence of "fireproof agents".
4. The mechanism of oxide film formation and its protection against ignition requires further detailed investigation.
5. The extra strengthening of flame-resistant magnesium casting alloys containing the LPSO phase is achieved through the solid-solution strengthening mechanism

Aknowledgement. The research was conducted with support from the Ministry of Science and Higher Education of the Russian Federation, Project FEMR-2020-0003.

References

1. N. V. Trofimov et al. Trudy VIAM: Elektron. Nauch.-Tekhn. Zh. 12 (48), 3 (2016). (in Russian) Crossref
2. J. Pezda, A. Jarco. Archives of Foundry Engineering. 16 (4), 95 (2016). Crossref
3. R. M. Pillai, K. S. B. Kumar, B. C. Pai. Journal of Materials Processing Technology. 146 (3), 338 (2004). Crossref
4. Magnesium alloys. Part 2: Guide (ed. by M. B. Altman, M. E. Driza et al.). Moscow, Metallurgiya (1979) 277 p. (in Russian)
5. Y. Kawamura, T. Marker. Flame-resistant magnesium alloys with high strength. The Seventh Triennial International Fire & Cabin Safety Research Conference. Philadelphia Marriott, Downtown (2013).
6. S. Inoue, M. Yamasaki, Y. Kawamura. Corrosion Science. 149, 133 (2019). Crossref
7. J. Kubásek et al. Journal of Alloys and Compounds. 877, 160089 (2021). Crossref
8. Y. Kawamura et al. Mater. Trans. 63, 118 (2022). Crossref
9. S. Inoue, K. Ishiage, Y. Kawamura. Journal of Alloys and Compounds. 934, 168014 (2023). Crossref
10. S. Inoue, M. Yamasaki, Y. Kawamura. Corros. Sci. 122, 118 (2017). Crossref
11. W. Wang et al. Materials Research Express. 6 (1), 016536 (2018). Crossref
12. S. Tekumalla, M. Gupta. Materials and Design. 113, 84 (2017). Crossref
13. W. Xuemin et al. Journal of Alloys and Compounds. 474 (1-2), 499 (2009). Crossref
14. L. L. Rohlin. Metal Science and Heat Treatment. 11, 18 (2006). (in Russian)
15. X. Zhang et al. Journal of Alloys and Compounds. 680, 212 (2016). Crossref
16. Z. Zhang et al. Materials & design. 88, 915 (2015). Crossref
17. S. Inoue, M. Yamasaki, Y. Kawamura. Corrosion Science. 174, 108858 (2020). Crossref
18. D. Han, J. Zhang, J. Huang et al. Journal of Magnesium and Alloys. 8, 329 (2020). Crossref
19. R. Kumar et al. Scripta Materialia. 49, 225 (2003). Crossref
20. N. Tahreen, D. L. Chen. Advanced Engineering Materials. 18 (12), 1983 (2016). Crossref